

# Results from the Commissioning of the n\_TOF Spallation Neutron Source at CERN

**C. Borcea, P. Cennini, M. Dahlfors, A. Ferrari, G. Garcia-Muñoz, P. Haefner  
A. Herrera-Martínez, Y. Kadi, V. Lacoste, E. Radermacher, F. Saldaña,  
V. Vlachoudis, L. Zanini**  
*CERN, CH-1211 Geneva 23, Switzerland*

**C. Rubbia**  
*University of Pavia, Pavia, Italy*

**S. Buono**  
*Advanced Accelerator Applications, Thoiry, France*

**V. Dangendorf, R. Nolte, M. Weierganz**  
*Physikalisch Technische Bundesanstalt, Braunschweig, Germany*

## Abstract

The new neutron time-of-flight facility (n\_TOF) has been built at CERN and is now operational. The facility is intended for the measurement of neutron induced cross sections of relevance to Accelerator Driven Systems (ADS) and to fundamental physics. Neutrons are produced by spallation of the 20 GeV/c proton beam, delivered by the Proton Synchrotron (PS), on a massive target of pure lead. A measuring station is placed at  $\approx 185$  m from the neutron producing target, allowing high-resolution measurements. The facility was successfully commissioned with two campaigns of measurements, in Nov. 2000 and Apr. 2001. The main interest was concentrated in the physical parameters of the installation (neutron fluence and resolution function), along with the target behavior and various safety-related aspects. These measurements confirmed the expectations from Monte Carlo simulations of the facility, thus allowing to initiate the foreseen physics program.

Geneva, Switzerland

25<sup>th</sup> October 2002

# Contents

<b>1</b>	<b>Introduction</b>	<b>1</b>
<b>2</b>	<b>The n_TOF facility</b>	<b>1</b>
<b>3</b>	<b>Experimental Setup and Measurements</b>	<b>2</b>
3.1	Detectors and DAQ . . . . .	2
3.2	Lead Target Behavior . . . . .	3
<b>4</b>	<b>Neutron Background</b>	<b>4</b>
<b>5</b>	<b>The neutron fluence</b>	<b>6</b>
5.1	Simulations . . . . .	6
5.2	Results from the fission chambers . . . . .	7
5.3	Results from the activation foils . . . . .	9
<b>6</b>	<b>The resolution function</b>	<b>10</b>
<b>7</b>	<b>Conclusions</b>	<b>12</b>
<b>8</b>	<b>Acknowledgments</b>	<b>12</b>

# 1 Introduction

The n\_TOF facility at CERN [1, 2, 3] is a high fluence spallation neutron source followed by a 185 m flight path. The aim of the n\_TOF project is the measurement of cross sections needed for the design of innovative ADS applications like incineration of nuclear waste [4, 5], energy production [6, 7], radioisotope production for medical applications [8] and basic science subjects, in particular astrophysics [1]. As a result of the studies reported in a first paper [2] and an addendum [3], the neutron time of flight facility has been proposed at the CERN PS [9] delivering a maximum intensity of  $3 \times 10^{13}$  protons within a 14.4 s supercycle at a momentum of 20 GeV/c. The facility allows to study systematically and with excellent resolution, neutron induced cross sections in the interval from thermal to hundreds of MeV, of almost any element using targets of very modest mass, necessary for the unstable or otherwise expensive materials.

In order to determine the physical parameters of the installation and compare them with the calculated ones, two campaigns of measurements have been carried out during the commissioning. A first phase took place in November 2000 and a second one in April 2001. While the main interest was concentrated on the physical parameters of the installation, the target behavior and various safety related aspects were also monitored. In the commissioning period two parallel plate ionization chambers with fissile deposits, one with  $^{235}\text{U}$  and another with  $^{238}\text{U}$ , were used. These detectors are inter-comparison instruments [10] and were provided by the Physikalisch-Technische Bundesanstalt (PTB). The present report will give a short description of the n\_TOF facility, followed by the experimental setup, measurements and the results compared with the simulations.

## 2 The n\_TOF facility

Following an overall optimization between neutron fluence  $\Phi$  and resolution  $\Delta\lambda$  ( $\lambda$  = effective neutron path), the spallation target was chosen to be a lead block of  $80 \times 80 \times 40 \text{ cm}^3$ , followed by a water moderator of 5 cm thickness [11]. In the final design [12] the neutron emission takes place at an angle of  $10^\circ$  with respect to the proton beam direction. The target is made of high purity (99.999%) lead shaped as a block of  $80 \times 80 \times 60 \text{ cm}^3$  with a special niche for the proton line. The target is immersed in water contained in an aluminum tank. A thin single metallic window (aluminum alloy) of 1.6 mm thickness is the interface between the moderator and the vacuum in the n\_TOF tube [12].

The horizontal time of flight tube (fig. 1) starts directly after the window and ends where the sloped floor of the TT2A tunnel (1.18% gradient) touches the tube, thus allowing a length up to 200 m. The pressure in the vacuum tube is less than 1 mbar. The tube is made up of four different sectors, the first one ( $\varnothing = 80 \text{ cm}$ ), closest to the target, is made of aluminum alloy whereas the others ( $\varnothing = 80, 60$  and  $40 \text{ cm}$ ) are made of stainless steel [12].

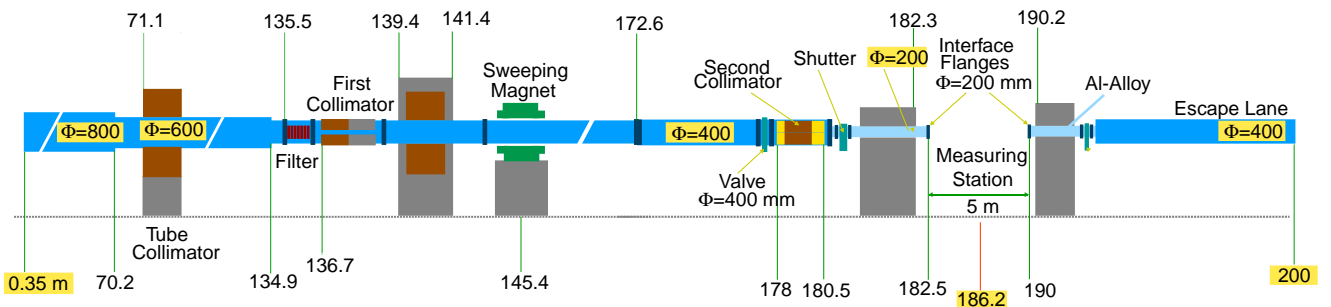


Figure 1: TOF tube sections up to the end of the TT2A tunnel (200 m).

In spite of the  $10^\circ$  angle between the time of flight tube and the proton beam, some charged particles

will remain and contaminate the neutron fluence. Therefore, a 2 m long dipole magnet, located at 145 m, is used to sweep away these unwanted secondary charged particles.

Two collimators [13] were installed to reduce the radius of the neutron beam, necessary for the capture measurements. The first one, 2 m long (beam shaping collimator) is located at 136.7 m and is made of 1 m of iron and 1 m of concrete; its inner diameter is  $\varnothing = 11.5$  cm. The second collimator (source screening collimator) with  $\varnothing = 1.8$  cm inner diameter, is placed at 178 m with 50 cm of 5% borated polyethylene, 125 cm of iron and 75 cm of 5% borated polyethylene. For the fission measurements, the second collimator will be replaced with one with a larger inner diameter of  $\varnothing \approx 8$  cm, in order to exploit the full neutron fluence of the installation.

Initially two concrete shielding walls of 2 m and 3.2 m respectively and a chicane were placed in the tunnel that lodges the time of flight tube to ensure proper background conditions. In September 2001 an iron wall of 3.2 m located at  $\sim 150$  m was added to reduce further the background, by diminishing the muon component which otherwise being stopped at the experimental area, produces a neutron background from negative muon captures [14].

All the measurements of the n\_TOF program are foreseen to take place under vacuum, however for the commissioning phase the vacuum tube was ended with a 500  $\mu\text{m}$ -thick aluminum window placed at a distance of 182.1 m from the window of the spallation target.

### 3 Experimental Setup and Measurements

#### 3.1 Detectors and DAQ

For the measurement of the neutron fluence in the energy range from thermal up to tens of MeV, and of the time resolution, we used ionization chambers with fissile deposits [10]. A parallel plate ionization chamber with  $^{235}\text{U}$  deposits was used for the measurement in the wide energy range, since the fission cross section for  $^{235}\text{U}$  is a standard up to 20 MeV. Additionally, another detector with  $^{238}\text{U}$  deposits was used. Both detectors were provided by PTB.

The detectors consist of five platinum cathodes with fissile deposits on both sides, separated by 5 mm from the anodes made of tantalum. The circular plates are 86 mm in diameter, and the fissile deposits have a diameter of 76 mm, thus wider than the neutron beam exiting the second n\_TOF collimator. The total masses of  $^{235}\text{U}$  and  $^{238}\text{U}$  are respectively  $(201.56 \pm 0.60)$  mg and  $(197.78 \pm 0.60)$  mg or equivalently  $(444 \pm 18)$   $\mu\text{g}/\text{cm}^2/\text{plate}$  for the  $^{235}\text{U}$  and  $(436 \pm 18)$   $\mu\text{g}/\text{cm}^2/\text{plate}$  for the  $^{238}\text{U}$ . The isotopic purity is about 99.9% for both deposits. The homogeneity of the deposits is of 4% for areas of 1  $\text{cm}^2$ . The overall thickness of the chambers is 50 mm, which work under atmospheric pressure, with a gas mixture made of 90% of Ar and 10% of  $\text{CF}_4$ . The detectors were enclosed in thin (150  $\mu\text{m}$ ) windows of tantalum. A scheme of the chambers is shown in fig. 2.

The detection efficiency of the  $^{238}\text{U}$  chamber is a slowly decreasing function of energy, and is about 95% in the energy range of interest. The  $^{238}\text{U}$  fission chamber was placed at a distance of 182.25 m and the  $^{235}\text{U}$  fission chamber at 182.35 m from the spallation target window.

The signals from the detectors were sent to the n\_TOF control room that hosted the data acquisition system (DAQ [15]) and the electronics. The DAQ has been specially elaborated for the commissioning measurements but it is a general purpose one. The DAQ concept stems from the necessity of preserving the time correlation of all the information coming from various detectors, sensors and monitors. Considering the high rates of events in the detectors induced by the proton burst, it was decided that a double system should be used: flash ADCs and multi-hit TDCs. The FADCs used was the model V676 from CAEN with 3 input channels, a sampling rate of 25 ns, and a buffer of 4096 samples, equivalent to 102.4  $\mu\text{s}$  sampling range. One FADC was used for each chamber, recording in the first channel the raw signal from the detector and on the second the discriminated from the CFD. The TDCs used were the model CAEN V767B, with 128 input channels, a time resolution of 0.8 ns and a buffer capable of recording up to 32k events. The active range of the TDCs is 800  $\mu\text{s}$ , but with a use of periodic signal

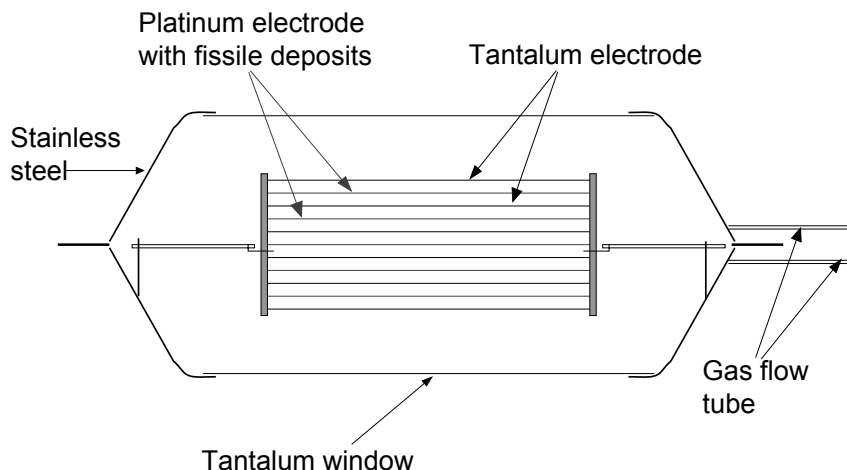


Figure 2: The multi-plate fission chamber from PTB.

of  $300 \mu\text{s}$  connected in one of the TDC channels, we could discriminate signals down to  $300 \text{ ms}$ , well below the thermal neutrons. One TDC was used for each detector, recording the arrival time of the discriminated signal from the CFD relative to the forerunning pulse from the PS. The threshold set on the CFDs was carefully chosen (fig. 3) to discriminate the alphas from the fission fragments.

Moreover, the DAQ was able to accommodate all the information coming from the beam transformers (for the intensity of the proton beam), beam profile monitors and thermocouples. The DAQ was triggered with the fore-running pulse from the PS. The measurements were performed in the first half of April 2001; a total number of  $8.6 \times 10^{17}$  protons were delivered by the PS in 155000 pulses with an average intensity of  $5.5 \times 10^{12}$  protons per pulse.

A large set of data was collected with the two fission chambers,  $3.17 \times 10^5$  events with the  $^{238}\text{U}$  fission chamber and  $6.57 \times 10^7$  events with the  $^{235}\text{U}$  fission chamber. Besides the fission chambers and as an alternative way of determining the neutron fluence at a specific energy, the double foil activation method was used. This method consists in the activation of two identical foils from the same material that has one large and isolated resonance. The two foils are overlapped and then activated together under the same neutron beam. The thickness of foils is chosen such that the first one (that sees the neutrons first) depletes entirely the fluence at the considered resonance energy, leaving the rest of the spectrum almost unchanged.

Gold foils were chosen as the neutron capture cross section of Au is a reference. In addition, gold has a large isolated resonance of about 27400 barns at 4.9 eV that creates very favorable conditions for applying the double foil technique. To avoid captures at thermal energies where the cross-section is also high, the two foils were wrapped in a cadmium shielding. In the data treatment [16], corrections were applied for the number of nuclei decayed during the irradiation, in between irradiation and measurement and during the gamma measurement itself. Moreover, care has been taken to correct for the detection efficiency and for the extended surface of the foils.

### 3.2 Lead Target Behavior

One important issue of the commissioning was the study of the target behavior. At full regime a maximum of four proton pulses per supercycle of 14.4 s, spaced by at least 1.2 s, are sent to the target. Considering that about half of the beam energy is deposited in the target [12], it results that about

3.2 kW are dissipated in the target, leading to a temperature increase and therefore requiring an adequate cooling. A special cooling station has been made for this purpose, having also filtering elements incorporated. Simulations have been performed in order to evaluate the temperature rise after the bursts. During the commissioning, the target temperature was monitored by thermocouples inserted inside the lead block in various positions. Fig. 4 shows the results of the temperature measurements done with the thermocouple placed in a region where the energy dissipation is maximum. The incident proton beam was displaced horizontally with respect to the central position and the regime was with four proton bursts per supercycle at nominal intensity. These measurements have been compared with simulations using a finite-element calculation [17].

The agreement between measurements and simulations is excellent. As shown in the fig. 4, the maximum temperature of the target at full regime is of about 90°C, which allows a reliable and safe operation of the facility. The temperature variation of the target as a function of time was also studied (fig. 5). The number of proton bunches per cycle was varied from one to four during the measurement. Each impact of the proton beam leads to an instantaneous temperature rise of about 7°C, followed by a decrease until the next bunch interacts with the target; the overall effect is a steady temperature rise up to the maximum value reached with four proton bunches per supercycle.

Another safety-related measurement concerned the activation of the target. Two months after the first commissioning period, the target was extracted from its container for visual inspection and radioactivity measurements. The dose measured in contact with the lateral walls of the target varied between 50 and 400  $\mu\text{Sv/h}$ . Two hot spots were detected: one where the protons entered the target (2.15 mSv/h) and another one in the center of the exit face (1.1 mSv/h).

## 4 Neutron Background

A background roughly two orders of magnitude higher than tolerable was found in the n\_TOF facility during the nTOF02 [18] experimental program. Detailed FLUKA simulations [19], revealed the production mechanism of the main background component. This was accounted to the negative muon captures

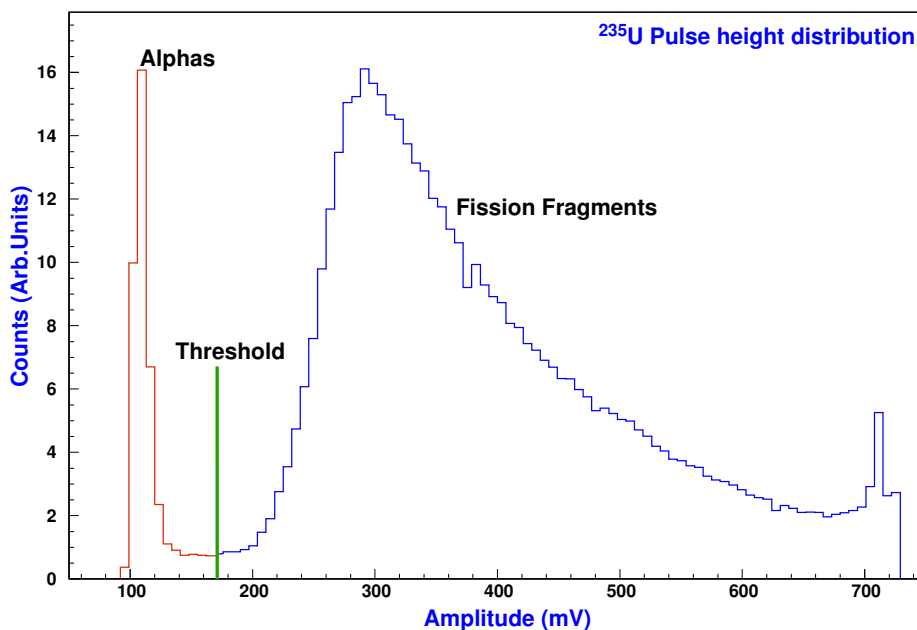


Figure 3: Pulse height distribution of the fission chamber detector with the  $^{235}\text{U}$  deposit. The discrimination threshold used on the CFD is also visible. The peak above 700 mV is due to saturation of the FADC module.

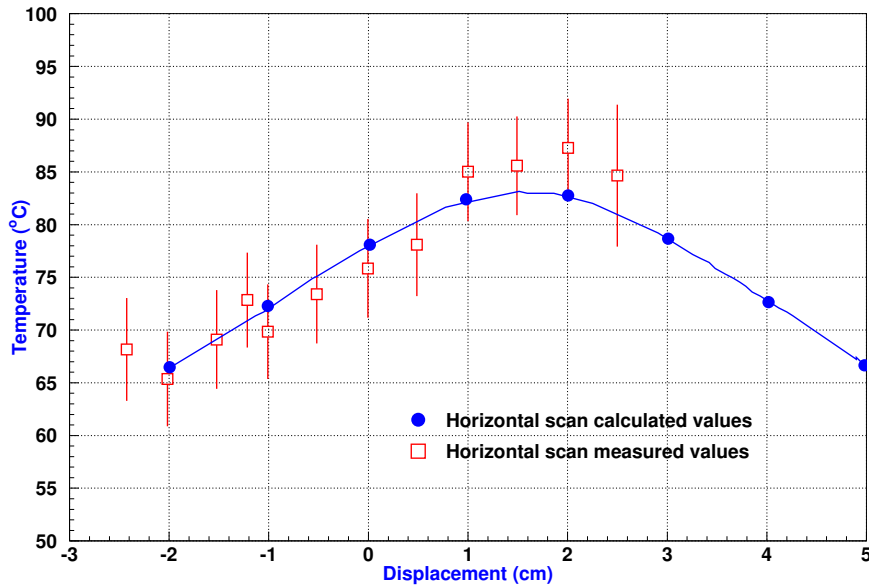


Figure 4: Temperature in the central thermocouple of the n\_TOF target during a horizontal beam scan.

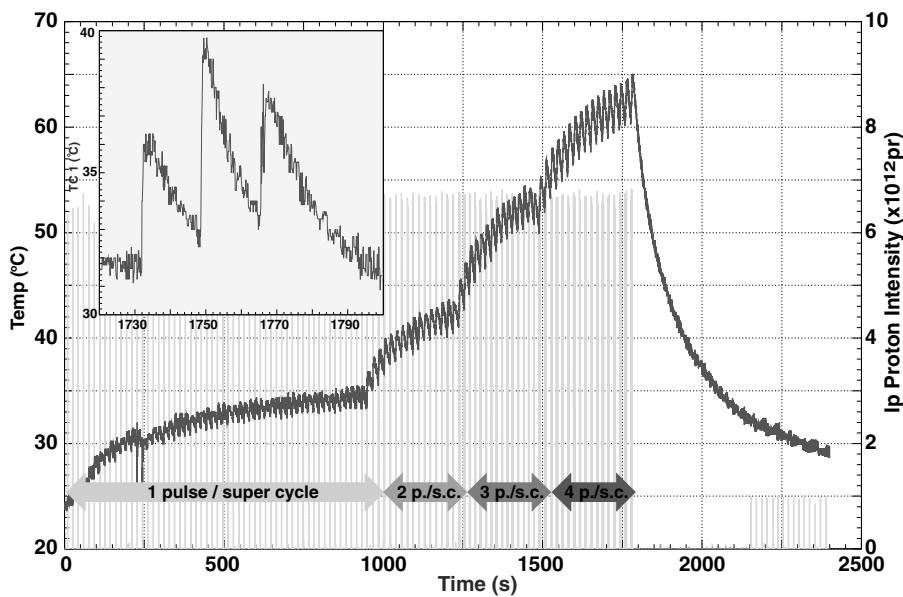


Figure 5: Temperature variation of the lead target. The measurement was done in a place close to the maximum energy deposit. On the right scale the proton intensity is indicated. The inset shows a detail on the instantaneous temperature jump at the impact of the proton pulse.

in the material surrounding the experimental area. The muons were the decay products of pions generated in the lead target from the spallation reactions. A first phase of measurements confirmed the results of the simulations, namely that the dominant source of background was due to neutrons generated by negative muon capture. Actions to reduce the background were taken according to the results from both measurements and simulations. A 3.2 m thick iron shielding wall was placed in between the sweeping magnet and the second collimator, with the purpose of stopping most of the muons. As reported in ref. [14], the ambient background was reduced by a factor of 30, leaving the sample related background the dominating component.

## 5 The neutron fluence

### 5.1 Simulations

One of the major tasks during the design phase of the n\_TOF facility was the simulation of the physical performances of the installation. Simulating geometries like the n\_TOF tunnel, with a long flight path, and with the imposed background conditions, is a very difficult and time-consuming task. To accomplish it, the most advanced computer codes FLUKA [20, 21, 22], EA-MC [23], MCNPX [24] have been used, coupled together whenever needed with specially written interfaces. Moreover, the accurate representation of the tunnel geometry used in the simulation codes was automatically generated with the use of in-house translators specifically made for this purpose, based on the civil engineering plans.

The simulation of the neutron fluence, one of the most important parameters of the facility, poses a serious difficulty due to the large length of the neutron flight path in the n\_TOF tunnel. The solid angle is so small that only one neutron out of  $\approx 10^7$  emerging from the lead target will reach the detector station at the end of the neutron tube. To solve this problem we separated the simulation process in two steps: *i*) simulation of the spallation target and generation of DST's (Data Summary Tapes) of the neutrons emerging from the aluminum window and entering in the neutron tube [25]; *ii*) geometrical transport of the previously collected neutrons in the neutron tube.

For the first step, two simulation codes were used, the intranuclear cascade code FLUKA and the Energy Amplifier Monte Carlo code EA-MC, with the detailed geometry of the lead spallation target, and its surroundings, including the modeling of the Al-window with the supporting grid. FLUKA was used for the production of neutrons with the spallation of the 20 GeV/c protons onto the solid lead target, and the transport of the generated neutrons down to the cut-off energy of 19.6 MeV. The transport of neutrons with kinetic energy below the cut-off of 19.6 MeV, was performed with the EA-MC code, where neutron induced interaction cross sections are available in the nuclear databases. All the neutrons emerging the lead target from the aluminum window with a direction lying in a cone with an aperture ( $\theta < 20^\circ$ ), heading toward the experimental area, were recorded into a DST file.

In the second step, the previously collected neutrons were transported geometrically towards the detector station into the neutron tube system. In the neutron transport we assumed a perfect collimation system: particles touching the collimators or the tube were killed. In order to enhance the statistics, we made the hypothesis that the direction of neutrons is isotropic within a small solid angle ( $\leq 10^{-7}$  sr). Thus, each particle was reused several times by changing slightly its direction, in such a way to scan an area of a few  $\text{cm}^2$  at the detector position. The program was scoring the number of occurrences of particles arriving at the detector plane for every position in the detector without touching any element of the neutron tube and collimators. The weight of each particle was properly normalized to reflect the number of times that it had been reused. The output histogram of this scanning procedure gave the integrated neutron fluence at the detector station.

The result of the fluence simulation is shown in fig. 6. The total number of neutrons entering the experimental area plotted in isoethargic units as  $dn/d\ln E/\text{cm}^2/7 \cdot 10^{12}$  pr is shown. On the same plot one can see also the simulation with MCNPX using a similar procedure like before, starting from the spallation of the protons on the lead target until the neutron transport to the detector area. The comparison of the various codes present a very good agreement, especially in the range from 1 eV to few MeV. At high energies, MCNPX shows a harder spectrum than what FLUKA is predicting. The difference in the high energy (larger than 100 MeV) part between the FLUKA and MCNPX spectra can be attributed to the use of an old version [26] of the FLUKA high energy interaction generator in MCNPX. The present version of FLUKA has undergone several major improvements/reworking along the years [20, 21, 22] which has vastly improved its performances when compared with available experimental data. The discrepancies in between 20 and 100 MeV could be still a consequence of the different high energy generator physics, or a genuine difference arising from the low and intermediate energy hadronic modelling in the two codes which are completely independent. On the other hand, MCNPX represents better the thermal



part when the  $S(\alpha, \beta)$  treatment is enabled for the light water, apart a few non-physical spikes which appear in the thermal peak, probably due to a binning effect. In the thermal region FLUKA shows the average of the only group that exists, and the EA-MC code is overestimating the effect of the thermal neutrons due to the absence of the  $S(\alpha, \beta)$  treatment for the light hydrogen inside the water moderator. A gravitational cut-off will occur due to the geometry of the beam pipe for neutrons with kinetic energies less than  $\approx 0.02$  eV.

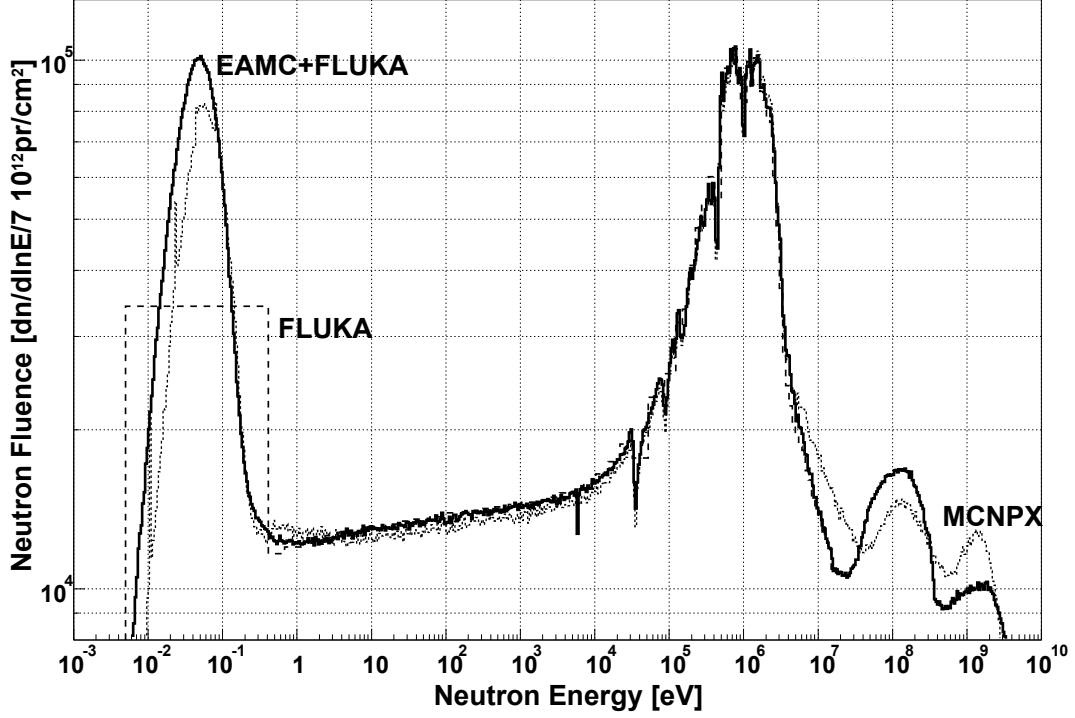


Figure 6: Monte Carlo simulation of the uncollimated neutron fluence at 200 m using different codes: combined FLUKA+EA-MC, FLUKA alone and MCNP-X.

## 5.2 Results from the fission chambers

The time-of-flight spectra obtained from the multi-hit TDC connected to each chamber were firstly corrected for the non-linearity of the TDC, determined from a measurement with a time calibrator, and then converted into neutron energy units, correcting also for the *effective neutron path*  $\lambda$  due to the moderation of the neutrons in the lead target [2, 3].

For the  $^{235}\text{U}$  chamber, data were obtained in the energy range from 0.01 eV up to 20 MeV. The detector was saturated for a few  $\mu\text{s}$  due to pile-up of the intense pulses detected in correspondence to the  $\gamma$ -flash, therefore it was not possible to measure at higher neutron energies.

Some corrections were needed to account for the fluence distortion induced by the  $^{238}\text{U}$  chamber, placed in front of the  $^{235}\text{U}$  fission chamber, and by the  $^{235}\text{U}$  chamber itself. If  $\Phi$  is the incident neutron fluence, the observed number of fission events in a given energy interval  $dE$  can be expressed in this particular situation as:

$$n_{fiss}(E)dE = \Phi(E)dE \times e^{-\sigma_{Pt}^{tot}n_{Pt}} \times e^{-\sigma_{Ta}^{tot}n_{Ta}} \times e^{-\sigma_{U238}^{tot}n_{U238}} \times e^{-\frac{\sigma_{U235}^{capt}n_{U235}}{2}} \left[ 1 - e^{-\sigma_{U235}^{fiss}n_{U235}} \right] + \Phi_B(E), \quad (1)$$

where the cross sections are in barns and the number of nuclei per barn  $n_i$  is used for the total amount of each specified material. The first three exponential factors account for the fluence decrease due to transmission through platinum, tantalum in both chambers and  $^{238}\text{U}$  layers contained in the first fission chamber. The fourth term accounts for the loss of fluence in the first half of the  $^{235}\text{U}$  chamber itself, due to its multi-layer structure. The last term accounts for the fission events occurring in the  $^{235}\text{U}$  chamber.

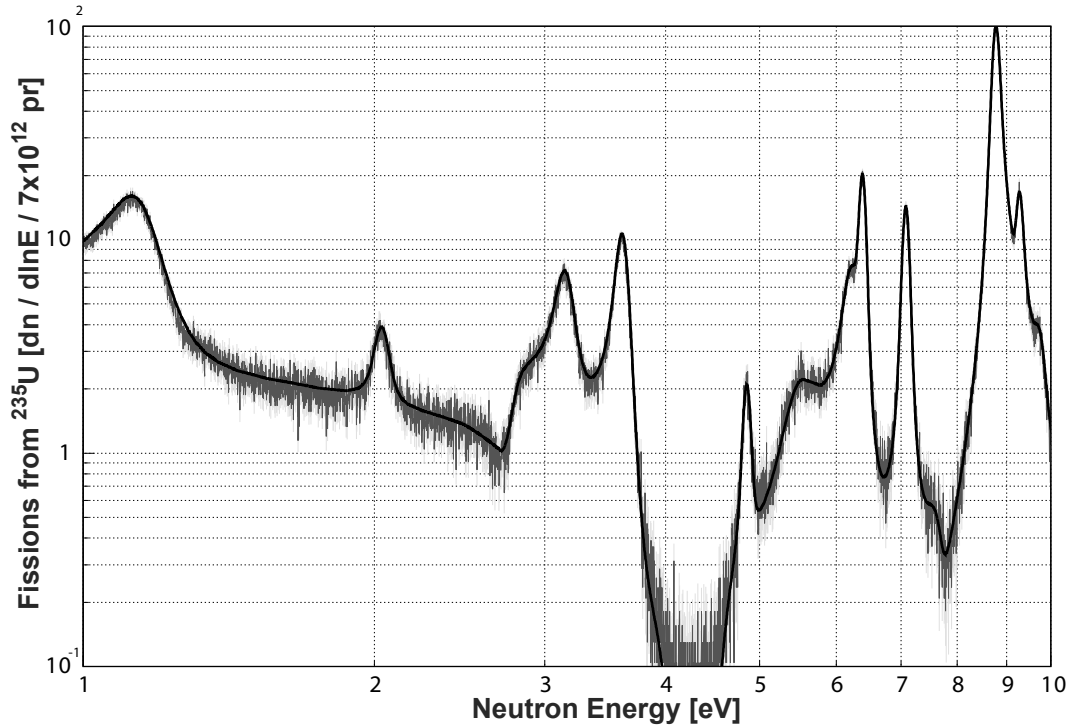


Figure 7: Experimental data obtained with the  $^{235}\text{U}$  fission chamber. The region from 1 to 10 eV is shown. The continuous line represents the ENDF/B-VI data scaled to match the experiment.

These corrections were determined using a recursive procedure, since the neutron fluence is not *a priori* known. However, these corrections are applicable both in the case of resonance absorption, as the fluence outside the resonance is assumed, and in the case of fluence decrease due to scattering of neutrons, if the scattering cross sections are known.

The results are shown in fig. 7 in the energy region between 1 and 10 eV. As shown, the agreement with the ENDF/B-VI Rel.6 database [27] is excellent. At some specific neutron energies the incident fluence may be completely depleted if in the transmission exponentials the cross section and/or the amount of material are large enough (*black resonances*). This is the case in particular for tantalum at 4.3 eV (see the deep valley in fig. 7).

On the other hand, the experimental data indicate that the valley is filled up to the level of 0.1 in the specified units. From this fact one may conclude about the presence of a background. The examination of other totally depleted zones (e.g. at 23.9 eV or 5.9 keV) showed that this background is constant in isoethargic representation, i.e.  $d\Phi_B(E)/d(\ln E)=0.1$ . Therefore its contribution has been added to the right hand side of eq. 1.

The measured incident neutron fluence is shown in fig. 8 together with the simulated one. One can observe the flat shape of the spectral function of n\_TOF in a wide energy domain, from 1 eV up to  $10^4$  eV, which confirms the expected isoethargic character. Some local depletions appear both in the simulated fluence and in the experimental data. They are due to the presence of various materials in the neutron beam, in particular the aluminum of the windows separating the target from the beam line and

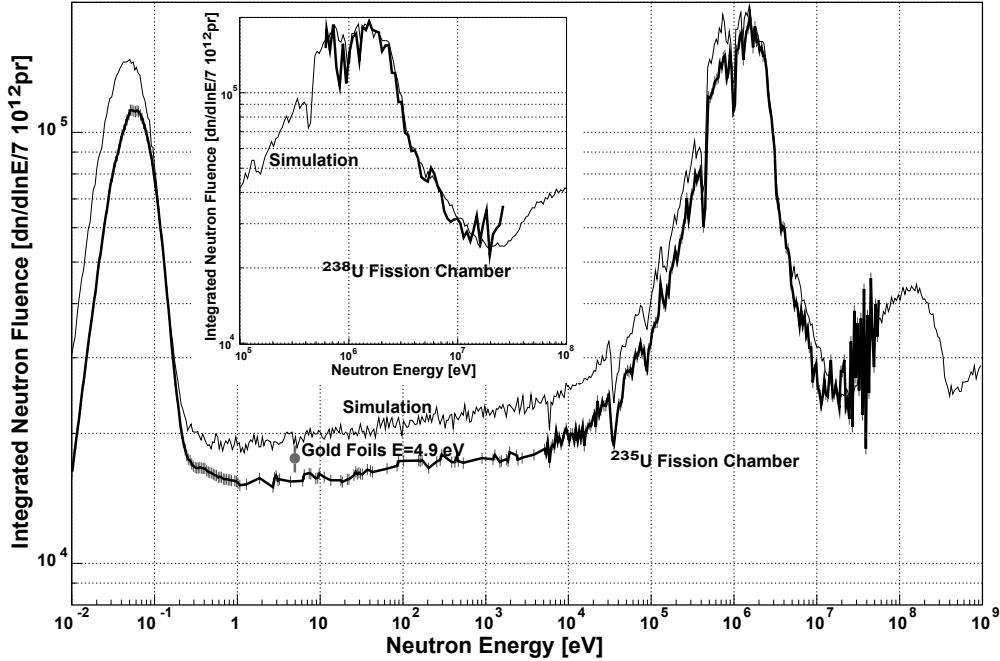


Figure 8: Neutron fluence as a function of energy from measurements with  $^{235}\text{U}$  and  $^{238}\text{U}$  fission chambers. The dashed curve represents the simulated fluence. The value of the fluence at 4.9 eV as determined by the activation of gold foils is also shown.

the one at the end of the neutron line and the oxygen contained in the 5 cm thick water moderator. In the high energy region (above 1 MeV) where the collimation effect is minimal the agreement between the simulated and the measured one is excellent. Below 1 MeV the measured data starts to deviate from the simulated one, establishing a maximum discrepancy of 20% for energies below  $\approx 100$  keV. This factor remains almost constant in the epithermal and thermal region, while the spectrum shape including all the resonances follows very closely the simulated one. For energies below 0.1 eV the gravitational cut-off affects the measured data while this effect is not included in the simulations. Considering the challenging problem of simulating a geometry like the n\_TOF tunnel, with all the assumptions used in such a simulation (beam profile, moderator thickness, windows, beam line components alignment, etc.), a discrepancy of 20% can be considered satisfactory.

A similar treatment was applied to the data of the  $^{238}\text{U}$  fission chamber. In this case, the corrective exponential factors in eq. (1) are less important, as this fission chamber was placed first. Moreover, the higher fission barrier of  $^{238}\text{U}$  (close to 1 MeV) makes this chamber insensitive to background neutrons of smaller energies than the threshold. The resulting neutron fluence is also shown in fig. 8 and is in excellent agreement with the  $^{235}\text{U}$  data.

### 5.3 Results from the activation foils

The gold foils labeled *A* and *B* were  $25\ \mu\text{m}$  in thickness and 4 cm in diameter. These samples, wrapped in a  $100\ \mu\text{m}$  thick cadmium shielding, were glued on the window of the  $^{238}\text{U}$  fission chamber. Foil *A* was placed toward the neutron beam. The foils were exposed to the neutron beam for 15 hours, for a total number of protons  $8.97 \times 10^{15}$ . After the activation the number of counts corresponding to the 411.8 keV  $\gamma$  line were measured separately for the two foils using a germanium detector. The number of  $^{198}\text{Au}$  nuclei produced by activation was obtained, and the neutron flux at 4.9 eV was deduced. The thickness of the foils was chosen such as to deplete entirely the fluence at the main resonance of 4.9 eV,

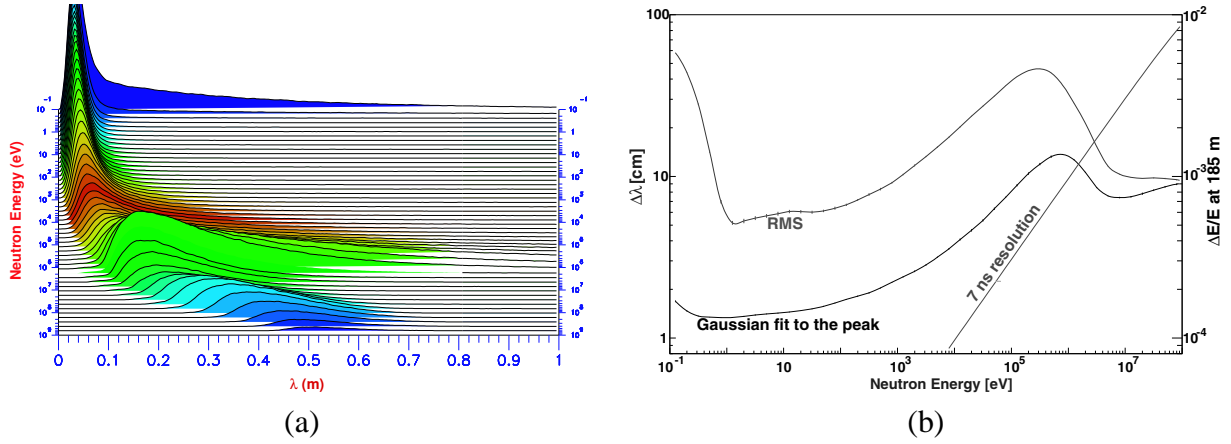


Figure 9: *a*) Monte Carlo distribution of the equivalent neutron path inside the moderator, evaluated at the energy of observation; *b*) Simulation of the energy resolution at 185 m. The 7 ns resolution due to the proton beam becomes dominant for neutron energies above a few MeV.

and leave the rest of the spectrum *almost* unchanged. The contribution of the rest of the spectrum due to the self shielding effect was estimated by means of simulation, to be of the order of 2%. This effect was applied as a systematic correction on the difference in the counts between the two foils.

Two separate activation measurements [16] were performed in Nov. 2001 and Apr. 2002. The two measurements agree with each other within the error bars. The combined integrated neutron fluence at the distance of 182.7 m and for  $7 \times 10^{12}$  incident protons is  $17500 \pm 1300$  neutrons at the resonance energy of 4.9 eV. This value is indicated in the fig. 8 for comparison with the fluence measurement done with the fission chambers. The results on the fluence with the activation foils is slightly higher than the one measured with the fission chambers by  $\approx 10\%$ . This higher value might be due to the presence of a directional neutron background [14] not considered in the evaluation.

## 6 The resolution function

Another goal of the commissioning phase of n\_TOF was to estimate the resolution function  $\Delta E/E$  of the facility. As indicated by the simulations [1], the energy resolution can be estimated using the relation

$$\frac{\Delta E}{E} = \frac{2\Delta\lambda}{\lambda + L} \quad (2)$$

between the energy  $E$  and the effective neutron path  $\lambda$  inside the lead followed by the 5 cm thick water moderator,  $L$  being the length of the flight path. This effective neutron path can be evaluated as  $\lambda = v \times t$ , where  $v$  is the neutron velocity when entering the neutron tube and  $t$  the time elapsed since its creation (fig. 9). The effective neutron path in the lead target is a few centimeters for the lowest energies; the variance  $\Delta\lambda$  has been evaluated taking either the r.m.s. of the  $\lambda$  distribution or the standard deviation from a Gaussian fit of the peaks.

The resolution  $\Delta E/E$  can be estimated by comparing the measured cross section with the database in correspondence of isolated, narrow resonances measured with high statistics.

In this spirit we have chosen to work on the  $^{235}\text{U}$  resonance at 7.1 eV. The first step was to convert the fission data collected with the chamber into cross section. This implies the knowledge of the neutron fluence and of the background. In addition, corrections for the absorbing elements (Pt, Ta) should be applied as indicated in eq. (1). In fact, this operation is the inverse one of the fluence determination described above. While the fluence determination was the result of a *global* operation (i.e. over the whole

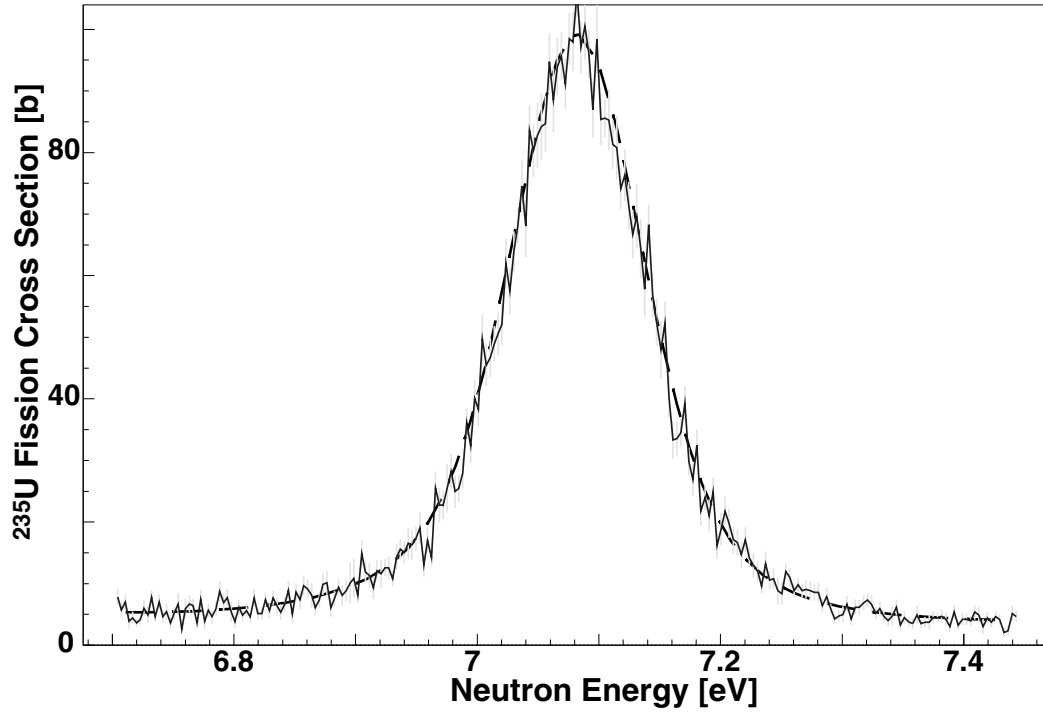


Figure 10: Experimental cross section from the  $^{235}\text{U}$  PTB Fission Chamber and ENDF-B/VI database.

energy domain), now we use the results obtained in a restricted energy domain around the resonance. This procedure is justified by the fact that the fluence is a flat function in the isoenergic representation, as shown in fig. 8.

The experimental cross section determined in this way is shown in fig. 10. Using the SAMMY code [28], two fits of the experimental cross section were performed. The first one had the aim to correct the position of the resonance that is shifted from the real energy due to the (unknown) effective neutron path correction  $\bar{\lambda}$  which has to be added to the flight path. The second fit was done to determine the fission channel width  $\Gamma_f$ . We obtained a value of  $\Gamma_{\text{exp}}=19.2$  meV whereas in the ENDF-B/VI database the channel width is  $\Gamma_{\text{db}}=18.12$  meV. The quadratic difference of the two values represents the r.m.s. broadening added to the width of the resonance due to the experimental resolution (the Doppler broadening was accounted for by SAMMY):

$$\Delta E = \sqrt{\Gamma_{\text{exp}}^2 - \Gamma_{\text{db}}^2} = 6.4 \text{ meV}, \quad (3)$$

where

$$\frac{\Delta E}{E} = \frac{2\Delta\lambda}{L + \lambda}. \quad (4)$$

Correspondingly, we deduced a value of  $9 \times 10^{-4}$  for the RMS of the  $\Delta E/E$  distribution, or a value of 8.2 cm for the RMS of the  $\Delta\lambda$  distribution.

This number provides only an upper limit for the resolution since it is limited due to the statistics and the assumptions about the background and neutron fluence done in the processing and the accurate knowledge of the support materials and fissile deposits. We have to stress also the fact that even though the measured value is comparable with the calculated r.m.s. value of the  $\Delta\lambda$  distribution obtained from simulations (fig. 9), it is only indicative of the real resolution that one can achieve with the n\_TOF facility. In fact, this estimation was done using a normal distribution for the  $\Delta\lambda$ , without handling

correctly the real shape of the resolution function. This shape, even if not known, can be approximated in a first iteration by the shape indicated by simulations.

## 7 Conclusions

Commissioning measurements have been performed for the n\_TOF facility at CERN. The main objectives were the determination of the neutron fluence and the resolution function of the installation. Both quantities were deduced from measurements with fission chamber detectors. The neutron fluence measured is in excellent agreement with the simulated one in the high energy region (above 1 MeV), while it differs at most by 20% with the values predicted by the Monte Carlo simulations in the epithermal region. This deviation can be considered reasonable, considering the challenges involved in the simulation of the n\_TOF facility. The measured fluence is isoethargic in the energy domain from 1 eV to 10 keV. The integrated neutron fluence at 182.5 m with the collimating system used in the commissioning was  $\approx 9.6 \cdot 10^5$  neutrons/ $7 \times 10^{12}$  protons. An independent measurement of the fluence at 4.9 eV by activation of gold foils gave results consistent with the ones of the fission chambers. The deduced resolution ( $\Delta E/E$ ) is better than  $9 \times 10^{-4}$  for neutron energy around 10 eV. These parameters allow performing high quality measurements for both astrophysical and ADS related cross sections.

## 8 Acknowledgments

The authors would like to thank the n\_TOF collaboration for their support and help during the commissioning period. We would also like to thank the CERN divisions SL, ST and accelerator people from PS.

## References

- [1] The n\_TOF Collaboration, *Proposal for a Neutron Time Of Flight Facility*, CERN/SPSC 99-8, SPSC/P 310.
- [2] C. RUBBIA *et al.*, *A high Resolution Spallation driven Facility at the CERN-PS to measure Neutron Cross Sections in the Interval from 1 eV to 250 MeV*, CERN/LHC/98-02 (EET).
- [3] C. RUBBIA *et al.*, *A high Resolution Spallation driven Facility at the CERN-PS to measure Neutron Cross Sections in the Interval from 1 eV to 250 MeV*, CERN/LHC/98-02 (EET)-Add .1.
- [4] C. RUBBIA *et al.*, *A Realistic Plutonium Elimination Scheme with Fast Energy Amplifiers and Thorium-Plutonium Fuel*, CERN/AT/95-53 (ET).
- [5] C. RUBBIA *et al.*, *Fast Neutron Incineration in the Energy Amplifier as Alternative to Geological Storage: the Case of Spain*, CERN/LHC/97-01 (EET).
- [6] C. RUBBIA *et al.*, *Conceptual Design of a fast Neutron Operated High Power Energy Amplifier*, CERN/AT/95-44 (ET).
- [7] C. RUBBIA, *A High Gain Energy Amplifier Operated with fast Neutrons*, AIP Conference Proceedings 346, International Conference on Accelerator-Driven Transmutation Technologies and Applications, Las Vegas, 1994.
- [8] C. RUBBIA, *Resonance Enhanced Neutron Captures for Element Activation and Waste Transmutation*, CERN/LHC/97-04.
- [9] R. BILLINGE, *The CERN PS Complex: A Multipurpose Particle Source*, Proc. of XIIth Intl. Conf. on High Energy Acc., 1983.

- [10] D.B. GAYTHER, *International Intercomparison of Fast Neutron Fluence-Rate Measurements Using Fission Chamber Transfer Instruments*, *Metrologia* 27 (1990) 221.
- [11] V. VLACHOUDIS and P. PAVLOPOULOS, *Optimization of the Lead Spallation Target Dimensions at the CERN Neutron Facility*, n\_TOF Int. Note 1998-02/BEAM.
- [12] Neutron TOF Facility (PS 213) , *Technical Design Report*, CERN/INTC/2000-004.
- [13] D.CANO-OTT and E.GONZALEZ *Proposal for a two-step cylindrical collimation system for the n\_TOF facility*, CIEMAT Ref: DFN/TR-04/II-00 (2000)
- [14] The n\_TOF Collaboration, *Study of the Background in the Measuring Station at the n\_TOF Facility at CERN: Sources and Solutions*, CERN/INTC 2001-038.
- [15] V. VLACHOUDIS, *A Multi Purpose DAQ System Developed for the n\_TOF commissioning*, In Proceedings of CHEP 2001, Edited by H.S.CHEN, Science Press New York, pg 562, 2001
- [16] V. LACOSTE *et al.*, *Neutron Flux measured by Activation of Gold Foils during the Commissioning of the n\_TOF Facility*, SL/EET Internal Note 004-2001.
- [17] S.BUONO, L.SORRENTINO, *Proposal of a set of measurements to take during the second commissioning phase of the TOF target in CERN*, CRS4/EA Internal Note 11, 22<sup>nd</sup> Mar. 2001
- [18] The n\_TOF Collaboration, *Determination of the neutron fluence, the beam characteristics and the background at the CERN-PS TOF Facility*, CERN/INTC 2000-016, 12 Feb. 2000
- [19] A. FERRARI, C. RUBBIA, V. VLACHOUDIS, *A Comprehensive study of the n\_TOF Background*, n\_TOF note 211009, SL-EET Note 2001-036.
- [20] A. FASSÒ, A. FERRARI, J. RANFT, P. R. SALA, G. R. STEVENSON and J. M. ZAZULA, *FLUKA92*, invited talk presented at the workshop on “Simulating Accelerator Radiation Environment”, SARE, Santa Fe, 11-15 January (1993), A. Palounek ed., Los Alamos LA-12835-C, p. 134-144 (1994).
- [21] A. FERRARI, and P.R. SALA, *The Physics of High Energy Reactions*, lecture given at the “Workshop on Nuclear Reaction Data and Nuclear Reactors Physics, Design and Safety”, International Centre for Theoretical Physics, Miramare-Trieste, Italy, 15 April–17 May 1996, Proceedings published by World Scientific, A. Gandini, G. Reffo eds, Vol. 2, p. 424-532, (1998).
- [22] G. COLLAZUOL, A. FERRARI, A. GUGLIELMI and P.R. SALA, *Hadronic models and experimental data for the neutrino beam production*, *Nuclear Instruments & Methods A*, **449**, 609-623 (2000).
- [23] Y. KADI *et al.*, *The EA-MC code package*, In Proceedings of the Fifth International Meeting on Simulating Accelerator Radiation Environment - SARE 5: Models and Codes for spallation neutron sources; OECD Headquarters, Paris, France, July 17-18, 2000.
- [24] H.G.HUGHES *et al.* *MCNPX for Neutron-Proton Transport*, Mathematical and Computation Topical Meeting, American Nuclear Society, Madrid Spain, Sept 27-30 1999.
- [25] V. VLACHOUDIS *et al.*, *Monte Carlo Simulation of the Neutron Time of Flight Facility at CERN*, In Proceedings of the Monte Carlo 2000 Conference, Lisbon, October 23-26 2000, A. Kling, F. Barão, M. Nakagawa, L. Távora, P. Vaz eds., Springer-Verlag Berlin, pg. 1175 (2001).
- [26] J. RANFT and S. RITTER, *Z. Phys.* **C27** (1985) 413, 569.
- [27] ENDF-B/VI, OECD NEA Data Bank (1996).
- [28] N. M. LARSON, *SAMMY: A Code System for Multilevel R-Matrix Fits to Neutron Data Using Bayes' Equations*, Oak Ridge National Laboratory Report No. ORNL/TM-9179/R4, 1998